Bull Volcanol (2006) 69: 175–187
DOI 10.1007/s00445-006-0066-5

RESEARCH ARTICLE

Bettina Scheu · Oliver Spieler · Donald B. Dingwell

Dynamics of explosive volcanism at Unzen volcano: an experimental contribution

Received: 25 August 2003 / Accepted: 10 March 2006 / Published online: 11 May 2006

Abstract Knowledge of the dynamics of magma fragmentation is necessary for a better understanding of the explosive behaviour of silicic volcanoes. Here we have measured the fragmentation speed and the fragmentation threshold of five dacitic samples (6.7–53.5 vol% open porosity) from Unzen volcano, Kyushu, Japan. The measurements were carried out using a shock-tube-based fragmentation apparatus modified after Alidibirov and Dingwell (1996a,b). The results of the experimental work confirm the dominant influence of porosity on fragmentation dynamics. The velocity of the fragmentation front increases and the value of the fragmentation threshold decreases with increasing porosity. Further, we observe that the fragmentation speed is strongly influenced by the initial pressure difference and the texture of the dacite. At an initial pressure difference of 30 MPa, the fragmentation speed varies from 34 m/s for the least porous sample to 100 m/s for the most porous sample. These results are evaluated by applying them to the 1990–1995 eruptive activity of Unzen volcano. Emplacements of layered lava dome lobes, Merapi-type pyroclastic flows and minor explosive events dominated this eruption. The influence of the fragmentation dynamics on dome collapse and Vulcanian events is discussed.

Keywords Fragmentation · Volcanology · Unzen volcano · Magma · Experiments · Porosity · Dome collapse · Vulcanian

Editorial responsibility: A. Woods

B. Scheu (✉) · O. Spieler · D. B. Dingwell
Earth and Environmental Sciences, University of Munich,
Theresienstr. 41/III,
80333 Munich, Germany
e-mail: scheu@eri.u-tokyo.ac.jp
Fax: +81-3-38129417

B. Scheu
Earthquake Research Institute, University of Tokyo,
113-0032 Tokyo, Japan

Introduction

The dynamics of the fragmentation of magma exerts a strong influence on the explosive behaviour and thus the eruptive style of a volcano (Dingwell 1996). The fragmentation speed, a hallmark of the eruption dynamics, is likely to be directly affected by the pressure distribution within the volcanic conduit or dome (Spieler et al. 2004a). The fragmentation threshold and the velocity of the fragmentation have been frequently discussed in conduit and eruption models, largely in the absence of any experimental data (e.g. Sparks 1978; Heiken and Wohletz 1991; Fink and Kieffer 1993; Alidibirov 1994; Sugioka and Bursik 1995; Kaminski and Jaupart 1998; Dingwell 1998b; Papale 1999; Zhang 1999; Melnik 2000; Alidibirov and Dingwell 2000).

In the past decade, several fragmentation and degassing experiments have been performed on analogous materials, e.g. H_2O–CO_2 polymer or gum-rosin-acetone systems (Mader et al. 1994, 1996); Phillips et al. 1995; Zhang et al. 1997). Experiments on viscoelastic silicone-oil derivatives represent a recent advance in the investigation of the physical behaviour of magma during expansion and fragmentation (Ichihara et al. 2002).

The first experiments on the fragmentation behaviour of natural magma under pressure were carried out with the fragmentation bomb built by Alidibirov and Dingwell (1996a,b). These experiments and subsequent studies of this nature have demonstrated that this technique can define several parameters that influence fragmentation in a wide variety of natural samples (Dingwell 1998a,b; Martel et al. 2000; Spieler et al. 2003, 2004a; Mueller et al. 2005).

In this paper, we present data on the speed of the fragmentation process in dacitic rocks of variable porosity from Unzen volcano, Japan. The experiments presented pertain to the brittle fragmentation process. Ductile fragmentation has also been discussed in the literature (Mader 1998; Dingwell 1998a; Cashman et al. 1999) as well as fragmentation caused by molten fuel coolant interaction (e.g. Zimanowski et al. 1997), analogous to phreatomagmatic events. We focus on brittle deformation in this paper, because this almost certainly caused the explosive erup-

tions of Unzen, as the high viscosity of Unzen lavas precludes ductile fragmentation (Dingwell 1996).

A primary driving force of the fragmentation process is the potential energy of the pressurized gas inside the vesicles of the magma. Thus, a higher overpressure is required to provide enough energy to overcome the strength of denser magma and cause fragmentation via layer-by-layer bursting of vesicles (Spieler et al. 2004b). In addition, at lower porosity, the inter-vesicle walls are stronger, assuming, to some extent, a random vesicle distribution. Clustering of vesicles may occur along degassing pathways during magma ascent. These clusters are, however, unlikely to have a distinct influence on the fragmentation behaviour on the scale of laboratory experiments, as they are locally very restricted and not sampled for experiments. However, they should be considered for the application of experimental results to broader scale eruption models.

For highly viscous magma, the layer-by-layer fragmentation is the most efficient and important of the three mechanisms proposed by Alidibirov and Dingwell (2000). The other mechanisms are fragmentation due to unloading wave or rapid filtration flow. Furthermore, we were able to prove that the porosity of magma is a key factor in controlling the explosive behaviour of a volcanic system (Spieler et al. 2004b).

During fieldwork at Unzen, we observed porosity layering inside large blocks of the pyroclastic flow deposits, as well as in the dome material (Figs. 4 and 5a). The existence of layered structures may be the sites for the initiation of the explosive events at Unzen. This paper highlights how such layering can influence the fragmentation behaviour. We produced a model for the speed at which a fragmentation wave propagates in a layered medium in order to explain fragmentation-induced collapse events and the Vulcanian explosions which occurred at Unzen.

Unzen eruption 1990–1995

Unzen volcano is located on the Shimabara Peninsula, Kyushu, Japan. The eruption started on 17 November 1990 with a small phreatic eruption, followed by phreatomagmatic explosions in February 1991. First lava extrusion occurred on 20 May 1991 and continued at changing effusion rates until February 1995. High effusion rate resulted in exogenous dome growth and low effusion rate in endogenous growth (Nakada et al. 1999). During this eruption, 13 lobes were extruded as result of exogenous dome growth forming a complex dome. The dome growth was accompanied by frequent pyroclastic flows and some minor explosive events. The majority and the most violent pyroclastic flows occurred at the initial stage during a period of high effusion rate; most of them were triggered by dome collapse events. An unexpectedly large pyroclastic flow led to 43 fatalities on 3 June 1991 (Nakada et al. 1999). Large dome collapse events resulted in vigorous pyroclastic flows on 8 June 1991 and 15 September 1991; the first of them was accompanied by explosions. Vulcanian explosions occurred in June and August 1991, the two largest on the 8 and 11 June 1991. The former was associated with a series of pyroclastic flows triggered by a collapse of big parts of the dome. The Vulcanian explosions were accompanied by shallow earthquakes located at a depth of about 500 m below the surface (Nakada et al. 1999). This may be the maximum depth reached by the fragmentation process (Goto 1999). Pumices produced during the Vulcanian explosions could only be found in the Peléan pyroclastic-flow deposits of June 1991 (Yanagi et al. 1992). Preceded by a seismic crisis, a second pulse of effusion occurred in February 1993, resulting in large pyroclastic flows during March to June 1993. The eruption finished in February 1995 with the extrusion of a spine at the endogenous dome (Nakada et al. 1999).

During the 1990–1995 activity, the SiO_2 content of the erupted magma remained nearly constant around 65 wt%. The erupted lavas are porphyritic and contain 23–28 vol% phenocrysts of plagioclase, hornblende, biotite and quartz. Plagioclase and hornblende exhibit the largest phenocrysts with average sizes up to 5 mm (Nakada and Motomura 1999). The groundmass is composed of rhyolitic glass (78–80 wt% SiO_2) and the groundmass crystallinity appears to be related to the magma ascent rate as it rises from 33 to 50 wt% with decreasing effusion rate (Nakada and Motomura 1999).

Petrological studies postulate a water content of 6 wt% for the pre-eruptive magma (Kusakabe et al. 1999; Botcharnikov et al. 2003). However, degassing during ascent decreased the water content of lavas to about 0.25 wt % in 1991 and to a negligible value in the later stage of the eruption. Kusakabe et al. (1999) measured water contents of 0.5 wt% in the chilled margin of breadcrust bombs and 0.3 wt% in their core; blocks from the dome also contained 0.3 wt% water. These values suggest that the magma degassed almost completely during slow ascent in the conduit. The degassing may have occurred either through wall rocks or through the magma column itself. The exsolved gas may have escaped through a relatively low-porosity, yet permeable, network of connected vesicles within the lava or have generated foamed lava whereby the foam collapsed before the lava reached the surface. Either process could have resulted in the extrusion of dense lava and the formation of a highly viscous dome.

Sample preparation

During two field campaigns, in 2000 and 2001, five blocks (approximately 40×40×9 cm), each with different porosity, were sampled from the 1991–1995 pyroclastic flow deposits of Unzen, most of them in the Mizunashi Valley. Up to 40 cylindrical samples of 25 mm diameter were drilled out of the sampled blocks for fragmentation experiments. The samples were cut and polished to a length of 60 mm with parallel ends. The open and closed porosity as well as the density were determined using a

helium pycnometer for all samples (Accupyc 1330, Micromeritics, USA). The mean density and porosity of each set of samples were calculated. The density scatter of the samples from each set was analysed and the samples with the smallest deviation were chosen for fragmentation experiments to ensure comparable initial conditions. The five blocks investigated here have open porosities of 6.7, 14.1, 20.5, 32.8 and 53.5 vol%, the highest porosity being from a breadcrust bomb. This porosity range covers the variation observed in the field very well (3.0–55.0 vol%; Kueppers et al. 2005).

Experiments

Experimental set-up

The fragmentation experiments were performed with a shock-tube-like apparatus (Alidibirov and Dingwell 1996a,b; Spieler et al. 2004a,b). The apparatus consists of two main parts: an autoclave (Fig. 1), in which the sample is slowly pressurized with Argon gas to up to 40 MPa, and a large tank, 3 m long and 0.4 m wide, at atmospheric pressure, in which the fragmented sample is collected. A system of three diaphragms separates the tank from the autoclave. The diaphragms open at certain overpressures and trigger the rapid decompression of the pressurized sample within the autoclave. When the unloading wave reaches the sample, a pressure gradient is created below the sample surface. Once a certain height and steepness of the gradient are overcome, the fragmentation of the sample ensues. The steepness of the pressure gradient is controlled by the initial pressure difference between the pressurized sample and the atmospheric conditions in the low-pressure tank, as well as the permeability of the sample (Mueller et al. 2005).

Previously, the sample size for fragmentation experiments was limited to cylinders of 50 mm length and 17 mm diameter. A newly modified autoclave now allows experiments to be performed on cylindrical samples of 60 mm length and 25 mm diameter.

Two dynamic pressure transducers (601H, Kistler Instrumente AG Winterthur, Switzerland) are used to quantify the speed of the fragmentation front travelling into the sample. These transducers are located directly above and below the sample (Fig. 1). As the operating temperature range of the transducers is 0–200 °C, the experiments are performed at room temperature. The speed of fragmentation is calculated from the distance between the pressure transducers and the time delay between the pressure drop above and below the sample. An additional static pressure transducer allows to monitor the slow and complete pressurization of autoclave and sample. Once the final pressure is reached, the sample remains under these conditions for 5–10 min. During this interval we assume that the smallest open pores are filled with argon gas, resulting in a homogeneous pressure distribution within the sample.

Experimental procedure

For each sample set, a series of experiments with increasing applied pressure were performed in order to determine the fragmentation threshold. The initial pressure applied to the sample in the first test was usually 2.0 MPa. If no fragmentation occurred, the initial pressure was raised by an increment of circa 1.0 MPa and the same sample was used for the next experiment. This process was continued

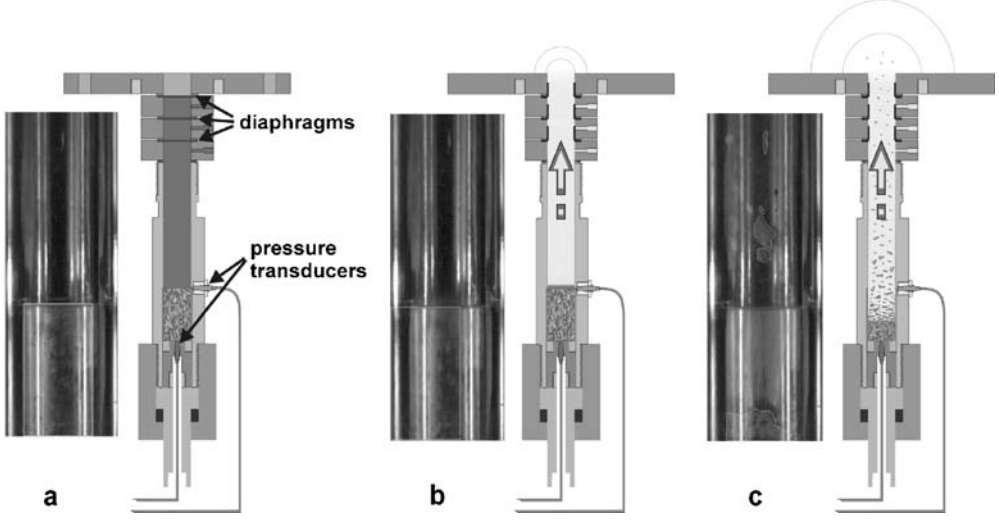

Fig. 1 The high-pressure autoclave is separated by three diaphragms from the low pressure tank. Two dynamic pressure transducers are installed directly above and below the sample to record the pressure drop curves during the rapid decompression of the autoclave and the sample. Modified still photographs on the *left* beside the drawings show the status of a sample at the different stages of the experiment. **a** The diaphragms are intact and the sample and the autoclave are slowly pressurized with Argon gas. **b** The diaphragms are broken and the unloading wave arrives at the sample and the first fine particles are blown out of the sample surface. The pressure gradient through the sample starts to build up. **c** The threshold of the sample is overcome and layer-by-layer fragmentation travels through the sample. In the modified still photograph the sample is already two thirds fragmented

Table 1 The average values of the fragmentation threshold of the five field samples

Sample name	Open porosity (%)	Fragmentation threshold (MPa)
MUZ 2001 A	6.7	20.5±2.5
MUZ 2000 D	14.1	14.0±1.2
MUZ 2001 C	20.5	10.0±1.0
MUZ 2000 G	32.8	7.5±1.0
BKB	53.5	4.0±0.5

until a first fragmentation occurred with, in most cases, a removal of only a few millimetres of the sample surface. This pressure is defined as the fragmentation initiation (FI). Usually, with about 0.5–1.5 MPa above FI, complete fragmentation of the sample is reached. This pressure is called the fragmentation threshold (FT). At pressures between FI and FT, only parts of the samples are fragmented. Either permeable flow through the sample apparently reduces the pressure gradient below FI, or a variation in the tensile strength within the sample, caused by natural inhomogeneities of the vesicle and crystal distribution increases FI. In any case, the energy provided by the compressed gas is not high enough to fragment another layer and the fragmentation stops. The remaining overpressure is reduced by permeable flow through the sample (see also Spieler et al. 2004a; Mueller et al. 2005).

Influence of experimental temperature

During the Unzen dome eruptions, the temperature of magma at fragmentation seemed to range between 800 °C down to a few hundred degrees Celsius. The highest fumarole gas temperature measured was around 800 °C (Nakada and Motomura 1999). During the initial stage of the eruption, surface temperature measurements, using an infrared thermal video system, revealed temperatures of around 550 °C at the dome and the active vent; a maximum temperature of 658 °C was measured at the dome in October 1991 (Umakoshi et al. 1992). The thermal imagery showed that at the front of a growing lava dome, temperatures were up to 300 °C, while in rock falls and pyroclastic flows, temperatures were between 110 and 280 °C.

The experiments presented here were performed at room temperature. A comparison of these threshold data with data gained at 850 °C revealed that the fragmentation threshold at low and high temperature is comparable within that range (Kueppers at al. 2005). Therefore the results are believed to be applicable to fragmentation over a wide range of temperature from room temperature up to eruptive temperature, as long as the fragmentation remains brittle.

Results

More than 100 experiments were carried out on five sample sets with differing porosities. For each sample set, first the fragmentation threshold was analysed as described above. The threshold was reproduced in several experiments and an average threshold was defined (Table 1). A characteristic selection of all experiments is listed in Table 2. We

Table 2 The fragmentation speed of the five analysed sample sets

Mean porosity (vol%)	Initial pressure (MPa)	Fragmentation speed (m/s)
6.7	10	No fragmentation
6.7	15	No fragmentation
6.7	17	No fragmentation
6.7	18	0
6.7	20	0
6.7	20	11.7
6.7	30	34
6.7	40	54
14.1	7	No fragmentation
14.1	9	No fragmentation
14.1	11	No fragmentation
14.1	12	No fragmentation
14.1	13	0
14.1	15	0
14.1	20	20
14.1	30	49.5
14.1	40	64
20.5	5	No fragmentation
20.5	6	No fragmentation
20.5	7	No fragmentation
20.5	8	No fragmentation
20.5	8.9	0
20.5	10	0
20.5	12	15
20.5	24	38.5
20.5	30	59
20.5	40	76.5
32.8	3.2	No fragmentation
32.8	3.4	No fragmentation
32.8	4.2	No fragmentation
32.8	5	No fragmentation
32.8	6.3	0
32.8	8.3	0
32.8	10	20
32.8	20	57.5
32.8	30	66.5
32.8	40	102
53.5	2.2	No fragmentation
53.5	3	No fragmentation
53.5	3.8	0
53.5	4.3	0
53.5	10	43
53.5	20	56
53.5	30	81
53.5	40	134

The data are plotted in Fig. 5a,b. Note: Not all experiments below threshold are mentioned here. The speed values are average values of several experiments

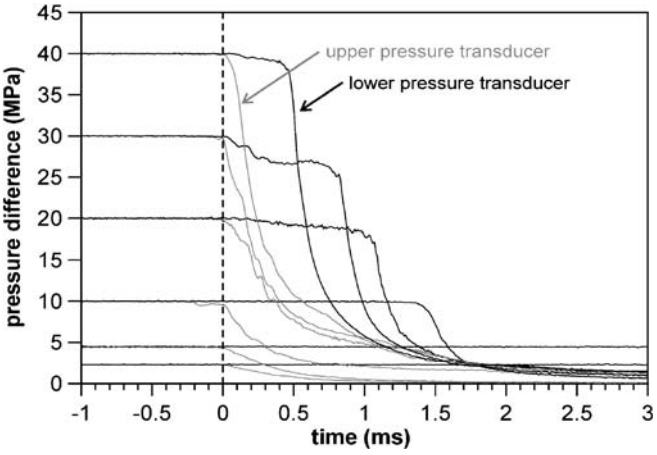

Fig. 2 Five experiments on one sample set (53.5 vol% open porosity) at different initial pressures. The pressure signals were recorded with two dynamic pressure transducers above and below the sample. The speed of fragmentation is calculated from the sample length and the time between the pressure drops at each end of the sample. The time decreases with increasing pressure

measured the speed of fragmentation for all sample sets at initial pressure differences, ΔP, of 10, 20, 30 and 40 MPa, as soon as the fragmentation threshold of the relevant sample set was overcome. At some sample sets, we conducted experiments at intermediate pressure differences in order to refine the observed speed curves. The fragmentation speed is calculated from the sample length (60 mm) and the time delay Δt of the pressure drop over the entire sample, as recorded by the transducers above and below the sample. Figure 2 shows pressure signals of the sample set with 53.5 vol% open porosity at several ΔP. With increasing ΔP, the time gap between the pressure drop above and below the sample decreases, i.e. the speed of fragmentation increases. Figure 3 displays the fragmentation speed for the five investigated varieties relative to the initial pressure; the corresponding data are listed in Table 2. The speed of fragmentation increases with increasing applied pressure. The strongest effect was observed at initial pressure values around FT. There is apparently a logarithmic relationship between the fragmentation speed and the initial pressure difference. At the maximum pressure applied to the samples (40 MPa), 6.7 vol% porosity resulted in a speed of 54 m/s and 52.2 vol% porosity gave 134 m/s. This appears to demonstrate that the speed is highly influenced by porosity, with an increase in porosity directly yielding an increase in the speed of the fragmentation process.

The intersections of the speed curves with the pressure axis in Fig. 3a (corresponding to a speed of 0 m/s) represent the fragmentation initiation for the different samples. Here it was decided to merge the values FI and FT, since it turned out that for a single sample one can very well distinguish between these values, whereas the natural inhomogeneity of the entire sample sets causes variations too wide to maintain such discrimination in a sensible manner. A mean FT value was defined, which is best understood as a range with the bandwidth given by the standard deviation (Table 1). A theoretical speed of 0 m/s was assigned to this (mean) FT. Their relative values reflect the strong influence of porosity on the threshold (Spieler et al. 2004b). The FT diagram of Fig. 3b also contains experiments performed at very low initial pressure (below FT), performed in order to obtain the fragmentation threshold for each sample set. Spieler et al. (2004b) described in detail the decrease of the fragmentation threshold with porosity, based on the results of high temperature experiments (850–900 °C).

Discussion

We have observed a clear dependence of fragmentation behaviour on porosity. An increasing porosity leads to a higher speed of fragmentation because more energy (gas expansion) is available. Also there is a smaller mass of rock to accelerate ahead of the fragmentation front, as well as a larger mass of gas with which to drive the acceleration of the ejecta. Furthermore, at a constant porosity, the fragmentation speed increases with increasing pressure due to a steepening of the pressure gradient, which also

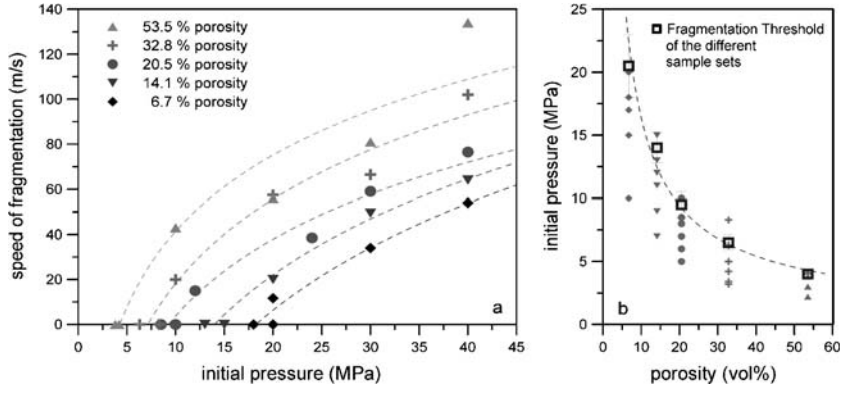

Fig. 3 **a** The speed of fragmentation and **b** the fragmentation threshold for the five sample sets with different porosity, which also contains the experiments below FT, performed to determine the fragmentation threshold. The experiments without fragmentation are marked with *small grey symbols*. The correlation between initial pressure and speed can be fitted using a logarithmic relationship. The correlation between the porosity and the threshold can be fitted with an inversely proportional exponential relationship

results in more energy available due to gas expansion. The energy E, which drives the fragmentation process, is largely provided by the expansion of the pressurized gas located in the pore space of the samples, therefore $E \sim \Delta P \bullet \Phi$, where Φ is the open porosity of the sample.

The speed data measured on a specific field sample exhibit a positive logarithmic dependence on the initial pressure difference, implicating an upper limit of the fragmentation speed. We postulate that the maximum speed is restricted by the sound speed of a pressurized dusty gas (Cagnoli et al. 2002), similar to a solid to gas mixture with the porosity of the analysed sample.

At a pressure range between FI and FT, or slightly higher, the fragmentation process is very sensitive to any kind of irregularity. Material heterogeneities can trigger a fragmentation below the average threshold of the sample, or prevent a fragmentation above this threshold.

The question may arise whether the repetitive pressurization and decompression of the same sample below FI influences the rocks strength. However, it turned out that repeated experiments at a pressure slightly below FI did not result in a lowered FT.

Implications for volcanic fragmentation

During a dome collapse or a sector collapse of a volcanic edifice, vesicular magma, pressurized due to lithostatic load and volatile diffusion, is exposed to rapid decompression. It depends on the properties of the magma whether a fragmentation occurs, leading to an explosive event. Dome lavas, for instance, are highly viscous and relatively degassed (Murase et al. 1985; Sato et al. 1992; Anderson et al. 1995).

In the following, several collapse and eruptions scenarios are introduced and applied to the 1990–1995 activity of Unzen. They are based on field observations and on results of the fragmentation analysis of vesicular magma in this study. Most of the introduced scenarios may occur combined during one eruptive cycle. The discussion of these scenarios is preceded by a section dealing with a very interesting field observation: a porosity layering, which bears direct implications for the proposed collapse models.

Porosity layering

During two field campaigns at Unzen volcano, we observed a porosity layering in large blocks of the pyroclastic flow deposits as well as on parts of the endogenous dome. Zones with high porosity may either be areas that were somehow protected from bubble collapse processes or are the result of a late gas exsolution event. Smith et al. (2001) mentioned cavitation, triggered by shearing of highly viscous magma, as a further possibility for their origin. We observed pressure shadows behind enclaves and shear fractures in large blocks of the pyroclastic flow deposits and at dome material (Fig. 4), supporting the notion of shear-driven cavitation. Finally, autobrecciation of large blocks during magma extrusion or slow flowing of the lobes is yet another process that could give rise to heterogeneously layered blocks. The zones of high porosity define bands, which appear to be caused by internal shearing parallel to the conduit wall during magma ascent (Tuffen et al. 2003; Gonnermann and Manga 2003; Kueppers et al. 2005; Kennedy et al. 2005). Banded blocks provide information on the internal structure of the dome, and as a result, the dispersion of a fragmentation wave inside such a layered medium needs to be considered in dome models.

Samples were drilled out of 11 layers of a large block with layered porosity variation (Fig. 5b). Density and open porosity of these samples were analysed using a helium pycnometer. The density values range from 1,630 to 2,370 kg/m^3 over the distance of several decimetres, according to an open porosity variation from 7.6 to 39.0 vol % (Fig. 5c). Hence these values cover the larger part of the porosity bandwidth observed at an extensive density mapping of the pyroclastic flow deposits and dome material after the last eruptive activity (Kueppers et al. 2005). This mapping revealed porosity values ranging from 3 to 49 vol%, not including breadcrust bombs. Not included in this range are breadcrust bombs ejected during

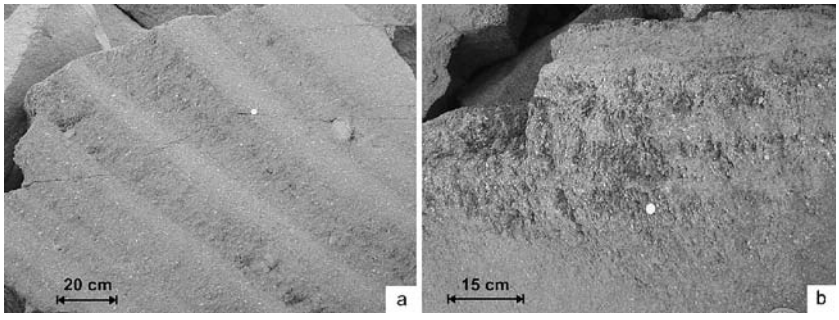

Fig. 4 Rock features observed at the endogenous dome of Unzen volcano. **a** A block with 5–10-cm-thick parallel layers of varying porosity. The layering may result from an internal shearing parallel to the conduit wall. In the uppermost layer (at the *right-hand side* of this picture) an 8-cm-large enclave with a pressure shadow can be seen. The *crack* running through all layers at an angle of about 30°–45° results from a subsequent event later than the layering, e.g. a cooling effect or shearing after the lava was solidified (or highly viscous). **b** This picture shows a porous area most likely generated by a cavitation process

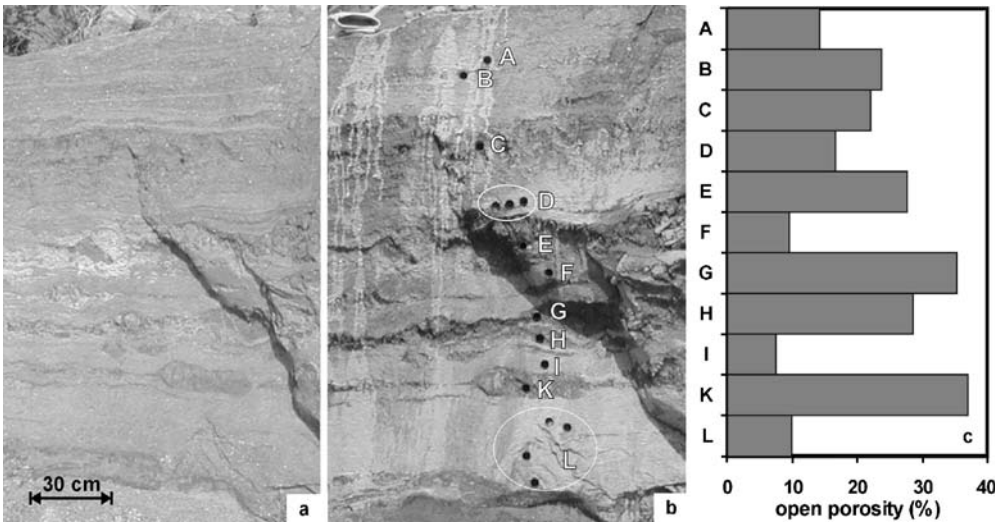

Fig. 5 Photos (**a**) and (**b**) show the same large layered block in the pyroclastic flow deposits of the 1990–1995 eruption of Unzen volcano before and after drilling. A portable diamond drill device was used to core samples out of the block to analyse the density variation and open porosity, respectively. **c** The graph shows the porosity variation of the layers in the block from top to bottom, as determined by helium pycnometry

the Vulcanian explosions. Their open porosity varies from between 40 and 55 vol%.

It is important to note that the sample, we took for density measurements and fragmentation experiments, simply represent the large grain-size fraction of the block and ash-flow deposits. A complementary fine fraction also exists. Importantly, we have found no evidence that these complementary coarse and fine fractions differ in initial porosity. Thus, they do not appear to be fed by different starting materials and, therefore, we must regard the obtained porosity range as representative of the pre-fragmentation porosity range in the respective Unzen domes from which they originated.

Fragmentation behaviour of a layered medium

Field evidence showed that the endogenous dome and the dome lobes of Unzen contain areas and layers with differing porosity. As observed in the fragmentation speed and threshold experiments of this study, the influence of porosity on the fragmentation behaviour is a lot. Thus, porosity changes in the dome must be taken into account as a first-order factor in eruption models.

Here, we use the layered block described above (Fig. 5) as a model for possible layering inside extruded dome lobes or magma in the upper conduit of Unzen. Then, we analyse the fragmentation behaviour of this block in several overpressure situations, using the fragmentation

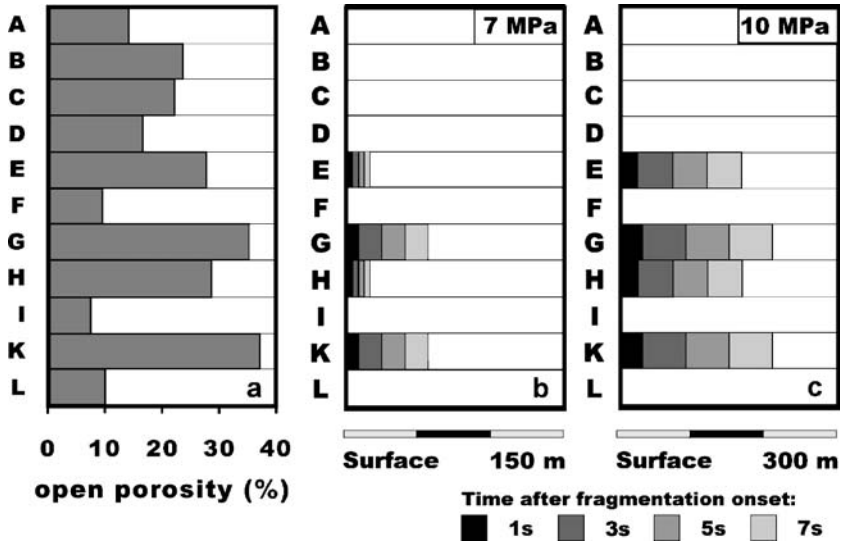

Fig. 6 **a** The porosity variation of the layered block (see also Fig. 5c) was used as a model to analyse the threshold and the speed distribution in a layered dome. **b** The fragmentation behaviour at 7 MPa overpressure. Four layers start to fragment. At layers *E* and *H*, the threshold is only slightly exceeded, which leads to a very slow fragmentation speed. For layers *G* and *K*, the pressure is well above the threshold. Here the fragmentation propagates 60 m into the dome in 7 s. **c** The fragmentation behaviour at 10 MPa overpressure. The same four layers as in Fig. 7 b start to fragment. In this case, the threshold of layer *E* and *H* is also clearly exceeded. After 7 s, the fragmentation wave has travelled 210 m into the most porous layers *G* and *K* and 160 m into the still highly porous layers *E* and *H*. The threshold of layers *B* and *C* is reached, but not overcome

threshold and speed values obtained for Unzen dacites (Fig. 3, Table 1).

First, we evaluated the response of that block to a pressure differential of 7 MPa (Fig. 6b). At the four most porous layers, the threshold is overcome and they start to fragment. The manner in which the fragmentation wave travels along the layers into the assumed dome is represented by bars for 1, 3, 5 and 7 s. Within layers E and H, the pressure is only slightly above FT; therefore, they fragment very slowly. Only the two most porous layers G and K are clearly above the fragmentation threshold. In these layers the fragmentation wave runs within 7 s 60 m deep into the medium, assuming steady conditions.

Figure 6c shows the fragmentation behaviour at a pressure difference of 10 MPa. As before, only at the four most porous layers E, G, H and K a fragmentation is initiated. However, in contrast to the situation at 7 MPa, here the threshold of all four layers is clearly exceeded. The fragmentation speed in all four layers is >20 m/s and thus the fragmentation front propagates in 7 s 160 m along layers E and H, and 210 m in the higher porous layers G and K. In the medium porous layers B and C, the internal pressure reaches the threshold, but FT is not overcome. These layers, therefore, should be in an unstable and weak condition and any further external perturbation may initiate a fragmentation or collapse.

Dome collapse events

In the following section, we discuss the implications of this layered model to several dome collapse scenarios, especially considering the last period of activity of Unzen volcano. The 1990–1995 eruption of Unzen was relatively quiet and non-violent compared to other dome-forming volcanoes such as Soufrière Hills volcano, Montserrat (Young et al. 1998; Sparks et al. 2002). The magma erupted at Montserrat is, in general, more porous with a higher total fraction of pumices, whereas the magma of Unzen degassed very efficiently during ascent and emplacement (mean density = 2,000 kg/m^3; Kueppers et al. 2005). Thus, in general, the high density and the reduced explosivity at Unzen are in good agreement with the experimental results documented in this study. Specifically it is consistent with the observation that the energy needed to fragment dense parts of the extruded lava lobes or the upper conduit of Unzen was too high to have been achieved by internal overpressure. The result was that most pyroclastic flows were triggered by gravitational dome collapse events, and only a few small volume Vulcanian eruptions occurred.

In some cases puffs of ash were noted just below the resulting collapse scar, directly preceding the crumbling of the blocks (Sato et al. 1992; Ui et al. 1999). This phenomenon may be interpreted as a locally restricted fragmentation event. Due to the internal pressure and maybe additional cooling tensions, the fragmentation threshold of a highly porous area or layer within the dome may be reached and the layer fragments. After a small fragmentation event due to a locally restricted overpressure situation, the overlying material becomes gravitationally destabilized and starts to crumble, inducing a pyroclastic flow (Fig. 7). Thus, the fragmentation of a small but highly porous layer may be sufficient to initiate a pyroclastic flow. The fragmentation might be arrested by a thinning out of the porous layer.

Compared to landslides, dome collapse events can last for a long time, even several hours or a day, consisting of different violent events. This happened, for example, during the last major dome collapse event at Montserrat in July 2003 (Carn et al. 2004). Also the large pyroclastic flow events in June–September 1991 and March–June 1993 at Unzen lasted at least several hours and consisted of a series of single events (Nakada et al. 1999).

During these long lasting events, a fragmentation may be triggered by the major or minor (gravitational) dome collapse. The collapse removes the outer parts of the dome, exposing a new surface of highly pressurized to ambient pressure conditions. For highly porous areas at the newly created surface, the fragmentation threshold may be exceeded and a fragmentation process is initiated (Fig. 8). The reduction of lithostatic load associated with dome collapse increases additionally the relative overpressure inside vesicles and thus enhances the likelihood of driving more fragmentation and collapse events. This may be one mechanism for keeping a collapse and pyroclastic flow event ongoing for several hours. The most violent and destructive pyroclastic flows at Unzen occurred at the end of a series of events (Nakada et al. 1999; Fujii and Nakada 1999). This seems reasonable, based on the mechanism proposed here. The fragmentation events and the associated pyroclastic flows become more violent towards the

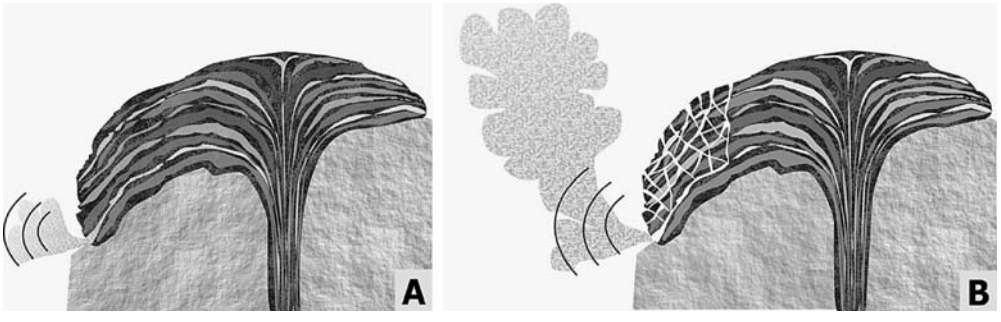

Fig. 7 A dome collapse scenario due to the fragmentation of a highly porous layer. **a** A highly porous layer within the dome lobe fragments due to the internal overpressure. **b** The fragmentation of the porous layer destabilizes the overlying part of the dome lobe causing it to collapse

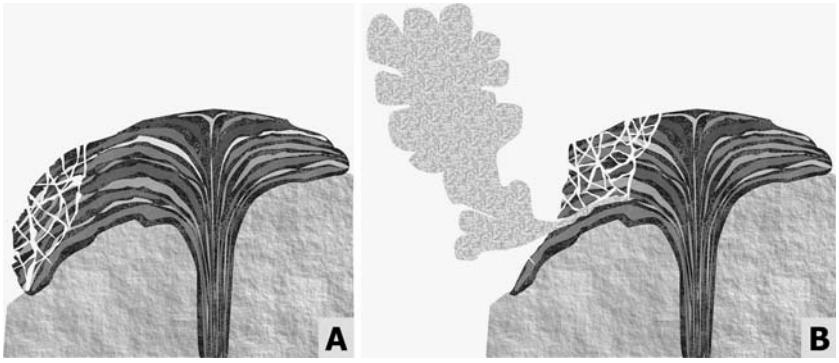

Fig. 8 Dome collapse scenario amplified by a fragmentation event. **a** A small gravitational dome collapse takes place and exposes more highly pressurized magma to the atmosphere. **b** On the newly exposed surface, the threshold of a highly porous layer is now overcome and the layer fragments. This fragmentation triggers the collapse of another part of the dome

central part of the dome as the pressure differential, which drives the fragmentation process, increases. At Montserrat, jets coming out of the rock face were observed after big dome collapses (R. Herd, 2003, personal communication). These jets can be interpreted as explosions caused by the collapse and probably related to decompression of small locally restricted areas, which is good proof for the proposed mechanism.

Vulcanian events

Observations of numerous dome-forming eruptions exhibit extended periods of effusive dome growth with intermittent short-lived explosive activity. During the effusive phase, degassed magma builds up a dome, while the exsolved volatiles filtrate through the permeable dome to the atmosphere (Eichelberger et al. 1986; Melnik and Sparks 1999). Field observations as well as models of dome growth have indicated that considerable overpressure, defined as pressure above local lithostatic pressure, can develop in such lava domes (Sato et al. 1992; Fink and Kieffer 1993; Melnik and Sparks 1999, 2002). Gas exsolution increases the viscosity of the magma by orders of magnitude and triggers crystallization, which can also increase the pressure in the upper parts of the conduit. Such overpressure at the base of a growing dome may reach several MPa and is dissipated by the escape of gas through the porous structure of the dome (Woods et al. 2002).

The pressure changes associated with a dome or sector collapse may be sufficient to initiate a Vulcanian explosion (Woods et al. 2002). For example, all Vulcanian explosions

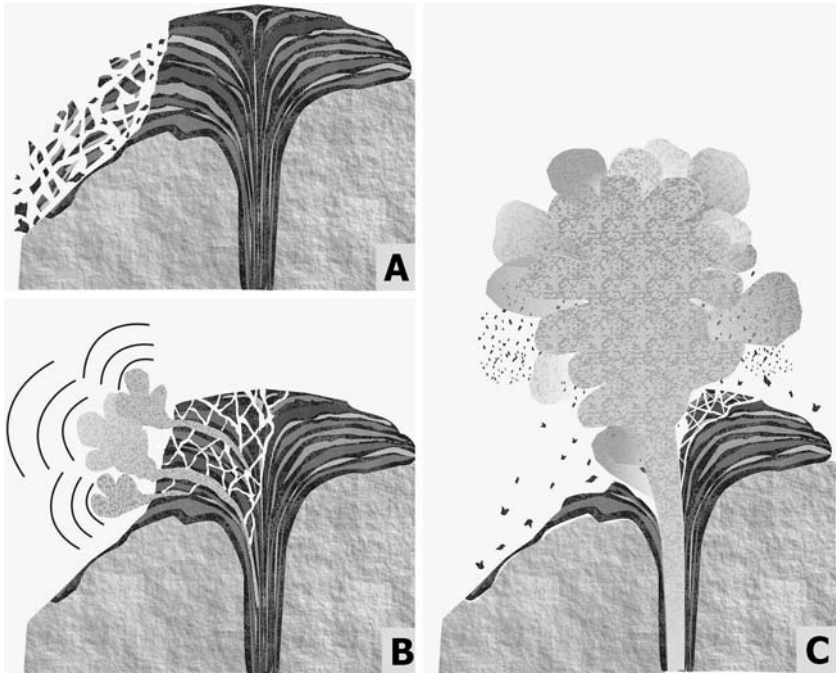

Fig. 9 A possible dome collapse scenario, amplified by a fragmentation event, leading to an explosive eruption. **a** A small gravitational dome collapse takes place and exposes more highly pressurized magma to the atmosphere. **b** On the newly exposed surface, the threshold of a few highly porous layers is overcome and these layers fragment. This fragmentation triggers the collapse of another part of the dome. If the fragmentation is not stopped by the punching out of the layer or a density increase within the layer, the fragmentation front may reach the conduit area. **c** A large dome collapse exposes highly pressurized magma to the atmosphere. This allows high-to-mid-porous magma to fragment, and the fragmentation propagates down into the conduit. An explosive event takes place and it depends on the magma properties within the conduit whether a Vulcanian or Plinian event occurs

during 1997 at Soufrière Hills volcano, Montserrat, were preceded by large dome-collapse events (Druitt et al. 2002), and also the Vulcanian explosions at Unzen volcano occurred after large pyroclastic flows and a landslide (Nakada et al. 1999).

A dome-collapse event may occur as indicated in Fig. 8, becoming increasingly vigorous with duration because, due to the retrograde movement of the new surface of the volcanic edifice, more and more highly pressurized magma is exposed. Again, for a few highly porous layers on this newly exposed surface, the threshold is overcome and these layers fragment. This fragmentation triggers the collapse of another part of the dome (Figs. 8, 9b). In case the fragmentation is not stopped by the punching out of the layer or a density increase within the layer, it may reach the conduit. This leads to another large collapse and the opening of the conduit. If the pressure difference is high enough, a fragmentation is initiated within the highly viscous conduit, usually leading to a Vulcanian explosion (Fig. 9c).

There are several other possible fragmentation scenarios, which we would like to describe briefly. If the ascent rate of a highly porous magma is comparable to the speed with which a fragmentation wave propagates down the conduit, a stable fragmentation surface may be established. At constant magma properties, this fragmentation would likely stabilize itself as follows. If the magma rose higher than the equilibrium fragmentation height and therefore decompressed more before fragmentation, an increased porosity would develop. This would cause the front to move back down the conduit due to the higher fragmentation speed at higher porosity. In contrast, a decreased porosity at fragmentation would exist if the magma fragmented below the equilibrium height (such that the magma had decompressed to less than the equilibrium height); in this case the magma might rise faster than the lower (downward) speed of the fragmentation front, leading to a return to equilibrium. Such a quasi-static equilibrium during sustained eruption might be the case for Plinian eruptions.

Additional changes of the properties of the uprising magma—e.g. due to slight variations in melt composition, crystal content or water—might generate variations in the degree of vesiculation at a constant depth level. Such variations might destabilize the fragmentation level in a manner as described in the following. A porosity decrease during an eruption reduces the gas expansion energy available for the fragmentation process and the ejection of the fragmented particles. One consequence could be a decrease in the fragmentation speed in the ascending magma and a rise of the fragmentation level. A porosity increase could result in the opposite effect, a higher propagation speed of the fragmentation front, a higher acceleration of the pyroclasts and the moving of the fragmentation level down the conduit. In combination, these effects could lead again to a pulsation, or, even cessation of the eruption.

Vulcanian events at Unzen

Two Vulcanian explosions at Unzen volcano occurred at an early stage of the eruption during the period of highest effusion rate. After rapid inflation of the summit area, first dome growth started on 20 May 1991. Large pyroclastic flow events took place on 3 and 8 June 1991, both associated with dome collapse events. The latter resulted in a collapse of two thirds of the dome, leading to a Peléan pyroclastic flow (Nakada et al. 1999). The removal of the upper part of a dome complex exposed magma with a higher pore pressure due to the lithostatic pressure. The resulting pressure gradient at the newly created surface may therefore have been high enough to fragment the porous magma within the vent. If this occurred, a fragmentation wave could start to propagate in this porous zone down the conduit, leading to a Vulcanian event (Fig. 9).

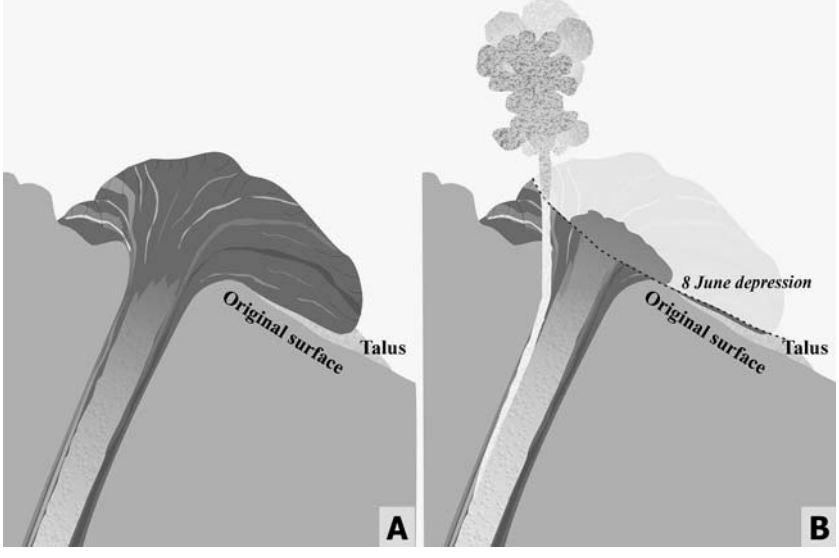

Fig. 10 A dome complex, fed by an inclined conduit. This complex is similar to the structure of Unzen volcano in June 1991. The inclined conduit and a fractured dome structure may have eased the Vulcanian eruption on 11 June 1992. **a** The inclined conduit allowed highly mobile, bubble-rich magma to accumulate at the roof of the conduit. **b** A major dome collapse on 8 June removed the upper part of the dome. The bubble-rich magma ascended along the top of the conduit and opened a fissure to the surface. The fissure may have been generated by shearing and cooling processes

On 11 June another Vulcanian event took place which was not accompanied by large pyroclastic flows. Nevertheless, it is very likely that this event was triggered or at least favoured by the removal of parts of the overlying dome by the preceding collapse event (8 June). A similar observation was made and successfully modelled at Soufrière Hills volcano, Montserrat, where a sub-Plinian explosion occurred a certain time after a big collapse, implicating unloading of the magma in the conduit as a causative key factor (Melnik and Sparks 2002). We propose a very similar mechanism leading to the 11 June Vulcanian event at Unzen. Magma that was still volatile rich started foaming in the conduit until the gas pressure overcame the yield strength of the magma (equivalent to the fragmentation threshold) and an explosion occurred. This event may have been the result of an isolated magma phase that was ascending slightly faster than the mean ascent rate of most extruded magma. This ascending magma phase seemed to have a lower viscosity than the average extruded lava, either due to a lower total crystallinity or, more probably, due to a higher water content or higher temperature. The magma may have ascended through fissures or shear cracks between the conduit walls and the host rock (Fig. 10). A slightly inclined conduit can be deduced from the location of the hypocenter region of volcanic tremor and LF earthquakes, which are related to the magma movement (Nakada et al. 1999; Umakoshi et al. 2001). The inclination of the conduit may have eased the rise of bubble-rich magma to the top of the conduit, similar to the idea proposed by Lane et al. (2001) for bubbly flow in inclined tubes. The location of the vent of this eruption, at the rim of the old crater (Nakada 1992), vertically above the inclined conduit supports this mechanism (Fig. 10). Since gas exsolution is less efficient at high ascent velocities, the water content in this magma remained higher than the mean water content of 0.25 wt% at the initial stage of the eruption. This is confirmed by Kusakabe et al. (1999), who measured a higher water content in the Vulcanian bombs; 0.5 wt% in the quenched rims and around 0.35 wt% in the cores.

The Vulcanian explosion on 11 June was accompanied by shallow earthquakes, located 500 m below the surface (Nakada et al. 1999; Goto 1999). This may be the maximum depth reached by the fragmentation process. The lithostatic pressure at this depth is 10 MPa, assuming a magma density of 2,000 kg/m^3. This corresponds to the pressure of the explosion calculated by Nakada et al. (1999) from the vertical velocity of the projectiles. Besides the lithostatic pressure, the excess pore pressure has to be taken into account, as due to the high viscosity of the Unzen magma, the bubble growth during depressurization is limited. Sparks (1978, 1994) pointed out that at high viscosities, on the order of 10^8 poise, an excess pore pressure of several MPa can be reached. Based on the viscosity and the water content of Unzen dacite, we assume an excess pore pressure of up to 5 MPa.

The experimentally determined fragmentation speed of the breadcrust bombs at around 10 MPa initial pressure difference is 40–50 m/s. Woods et al. (2002) assumed a fragmentation speed of 10 m/s for the Vulcanian events at Montserrat, which seems to be very slow, taking the higher porosity of the ejecta at Montserrat into account. Based on our experimental results, we can deduce that the time needed for the fragmentation front to reach a depth of 500 m is about 10–12.5 s. The volume of the ejected material was estimated by Nakada et al. (1999) to be 3–6×10^4 m^3. As a first order approximation, this would represent a cylinder 500 m in length with a radius of 3–4 m; or a dyke-like conduit area of about 2×30 m in width and 500 m in depth, taking a dyke shaped structure of the conduit into account, as suggested by the results of the Unzen scientific Drilling Project (Nonaka et al. 2004; Nakada et al. 2004).

There appears to be several different ways to stop the fragmentation process. Firstly, the fragmentation may loose momentum and slow down as the magma gradually becomes denser or less foamed. Secondly, a batch of foamed magma, whose volume might be restricted in some way, may be blown out completely and the fragmentation will cease quite sharply by entering the denser surrounding magma or wall rock. Furthermore, the fragmentation may stop if the conduit becomes choked, because the volume of gas in the vesicles is insufficient to propel the pyroclasts out of the conduit. Finally, small-scale "lateral fragmentation" at the sidewalls of the vent during a Vulcanian eruption may plug it up (Kennedy et al. 2005).

Summary

The style and progression of an eruption depends on the properties of its vesicular magma. If its fragmentation threshold can be exceeded, an explosive event may take place. Otherwise the magma is extruded quiescently in a dome-forming eruption.

This study comprises a detailed investigation of the fragmentation behaviour (threshold and propagation speed) of differently porous sample sets from Unzen, Japan. The experiments were performed with a shock-tube-based fragmentation apparatus and pertain to the brittle fragmentation process. Our results show a strong influence of the open porosity and the initial pressure on the fragmentation behaviour. We observed fragmentation speed values ranging from 12–134 m/s for applied pressure differences of up to 40 MPa and open porosities from 6.7–53.5%.

We applied the fragmentation results to the dome-collapse events and Vulcanian events of the 1990–1995 Unzen eruption. Large blocks with layers of varying porosity were observed at the pyroclastic flow deposits of Unzen volcano and support the model that a dome and dome lobes consist of areas of differing porosity. A layered composition of a dome and dome lobes, respectively, may lead to the fragmentation of single layers, followed by the

collapse of the overlaying sections. These events could catalyze gravitationally induced dome-collapse events leading to vigorous pyroclastic flows and/or trigger a sector collapse followed by a Vulcanian event.

The slow magma ascent and extrusion rate at Unzen resulted in relatively dense extruded magma, as the magma could almost completely degas during the ascent. The low porosity of this magma causes a high fragmentation threshold of most material, which is too high for unassisted fragmentation. Therefore, dome collapse events were the most abundant events of the 1990–1995 activity of Unzen volcano, leading to numerous pyroclastic flows. Also, the fragmentation-amplified collapse of dome lobes or parts of the dome seems to be reasonable. This accounts especially for the long lasting collapse events with vigorous pyroclastic flows at the early stage of the eruption in June 1991, which were followed by minor Vulcanian events. Nevertheless a larger explosive event, triggered by a landslide or a sector collapse of the dome, would have been possible.

Acknowledgements This work was partially funded by the project DI 431-20-1 from the German Science Foundation (DFG). The fieldwork and sampling were carried out in 2000 and 2001 together with Ulrich Kueppers. Joachim Gottsmann (Institute of Earth Sciences "Jaume Almera", Barcelona, Spain) drilled the layered block during the 2000 field campaign. We would like to thank Ben Kennedy, Ulli Kueppers, Sebastian Mueller and Alex Nichols for helpful discussions, Setsuya Nakada and Hiroshi Shimizu for providing us with qualitative information. Shimabara Earthquake and Volcano Observatory (SEVO) permitted access to the Unzen National Park and provided logistic support during fieldwork. Two anonymous reviewers and Andy Woods contributed helpful suggestions that improved the manuscript.

References

Alidibirov M (1994) A model for viscous magma fragmentation during volcanic blasts. Bull Volcanol 56:459–465

Alidibirov M, Dingwell DB (1996a) Magma fragmentation by rapid decompression. Nature 380:146–148

Alidibirov M, Dingwell DB (1996b) An experimental facility for investigation of magma fragmentation by rapid decompression. Bull Volcanol 58:411–416

Alidibirov M, Dingwell DB (2000) Three fragmentation mechanisms for highly viscous magma under rapid decompression. J Volcanol Geotherm Res 100:413–421

Anderson SW, Fink JH, Rose WI (1995) Mount St. Helens and Santiaguito lava domes: the effect of short-term eruption rate on surface texture and degassing processes. J Volcanol Geotherm Res 69:105–116

Botcharnikov R, Holtz F, Behrens H, Sato H (2003) Phase equilibrium study and constraints on pre-eruptive conditions of Unzen magmas. Abstract volume of Schwerpunktkolloquium IODP-ICDP, University of Hamburg, Hamburg, 3 pp

Cagnoli B, Barmin A, Melnik O, Sparks RSJ (2002) Depressurization of fine powders in a shock tube and dynamics of fragmented magma in volcanic conduits. Earth Planet Sci Lett 6419:1–13

Carn SA, Watts RB, Thompson G, Norton GE (2004) Anatomy of a lava dome collapse: the 20 March 2000 event at Soufrière Hills volcano, Montserrat. J Volcanol Geotherm Res 131:241–264

Cashman KV, Sturtevant B, Papale P, Navon O (1999) Magmatic fragmentation. In: Sigurdsson H, et al. (eds) Encyclopaedia of volcanoes. Academic Press, San Diego, pp 421–430

Dingwell DB (1996) Volcanic dilemma: flow or blow? Science 273:1054–1055

Dingwell DB (1998a) Recent experimental progress in the physical description of silicic magma relevant to explosive volcanism. In: Gilbert JS, Sparks RSJ (eds) The physics of explosive volcanic eruptions. Geol Soc Lond Spec Publ 145:9–26

Dingwell DB (1998b) Magma degassing and fragmentation: recent experimental advances. In: Freund A, Rosi M (eds) From magma to tephra. Modelling physical processes of explosive volcanic eruptions. Developments in volcanology. Elsevier, Amsterdam, pp 1–23

Druitt TH, Young SR, Baptie B, Bonadonna C, Calder ES, Clarke AB, Cole PD, Harford CL, Herd RA, Luckett R, Ryan G, Voight B (2002) Episodes of cyclic Vulcanian explosive activity with fountain collapse at Soufrière Hills Volcano, Montserrat. In: Druitt TH, Kokelaar BP (eds) The Eruption of Soufrière Hills Volcano, Montserrat, from 1995 to 1999. Geol Soc Lond Mem 21:281–306

Eichelberger JC, Carrigan HR, Westrich HR, Price RH (1986) Nonexplosive silicic volcanism. Nature 323:595–602

Fink J, Kieffer SW (1993) Estimate of pyroclastic flow velocities resulting from explosive decompression of lava domes. Nature 363:612–615

Fujii T, Nakada S (1999) The 15 September 1991 pyroclastic flows at Unzen Volcano (Japan): a flow model for associated ash-cloud surges. J Volcanol Geotherm Res 89:159–172

Gonnermann HM, Manga M (2003) Explosive volcanism may not be an inevitable consequence of magma fragmentation. Nature 426:432–435

Goto A (1999) A new model for volcanic earthquake at Unzen Volcano; melt rupture model. Geophys Res Lett 26(16):2541–2544

Heiken G, Wohletz K (1991) Fragmentation processes in explosive volcanic eruptions. In: Fisher RV, Smith G (eds) Sedimentation in volcanic settings. Soc Sediment Geol Spec Pub 45: 19–26

Ichihara M, Rittel D, Sturtevant B (2002) Fragmentation of a porous viscoelastic material: implications to magma fragmentation. J Geophys Res 107(B10):2229, DOI:10.1029/2001JB000591

Kaminski E, Jaupart C (1998) The size distribution of pyroclasts and the fragmentation sequence in explosive volcanic eruptions. J Geophys Res 103:29759–29779

Kennedy B, Spieler O, Scheu B, Kueppers U, Taddeucci J, Dingwell DB (2005) Conduit implosion during Vulcanian eruptions. Geology 33(7):581–584

Kueppers U, Scheu B, Spieler O, Dingwell DB (2005) Field based density measurements as tool to recalculate pre-eruption dome structure: set-up and first results. J Volcanol Geotherm Res 141:65–75

Kusakabe M, Sato H, Nakada S, Kitamura T (1999) Water contents and hydrogen isotopic ratios of rocks and minerals from the 1991 eruption of Unzen volcano, Japan. J Volcanol Geotherm Res 89:231–242

Lane SJ, Chouet BA, Phillips JC, Dawson P, Ryan GA, Hurst E (2001) Experimental observations of pressure oscillations and flow regimes in an analogue volcanic system. J Geophys Res 106:6461–6476

Mader HM (1998) Conduit flow and fragmentation. In: Gilbert JS, Sparks RSJ (eds) The physics of explosive volcanic eruptions. Geol Soc Lond Spec Publ 145:51–71

Mader HM, Zhang Y, Phillips JC, Sparks RSJ, Sturtevant B, Stolper E (1994) Experimental simulations of explosive degassing of magma. Nature 372:85–88

Mader HM, Phillips JC, Sparks RSJ, Sturtevant B (1996) Dynamics of explosive degassing of magma: observations of fragmenting two-phase flow. J Geophys Res 101:5547–5560

Martel C, Dingwell DB, Spieler O, Pichavant M, Wilke M (2000) Foaming and fragmentation in silicic melts: an experimental study. Earth Planet Sci Lett 178:47–58

Melnik OE (2000) Dynamics of two-phase conduit flow of high-viscosity gas-saturated magma: large variations of sustained explosive eruption intensity. Bull Volcanol 62:153–170

Melnik O, Sparks RSJ (1999) Nonlinear dynamics of lava dome extrusion. Nature 402:37–41

Melnik O, Sparks RSJ (2002) Modelling of conduit flow dynamics during explosive activity at Soufrière Hills Volcano, Montserrat. In: Druitt TH, Kokelaar BP (eds) The eruption of Soufrière Hills Volcano, Montserrat, from 1995 to 1999. Geol Soc Lond Mem 21:307–317

Mueller S, Melnik O, Spieler O, Scheu B, Dingwell DB (2005) Permeability and degassing of dome lavas undergoing rapid decompression: an experimental determination. Bull Volcanol 67:526–538

Murase AR, McBirney T, Melson WG (1985) Viscosity of the dome of Mount St. Helens. J Volcanol Geotherm Res 24:193–204

Nakada S (1992) Lava domes and pyroclastic flows of the 1991–1992 eruption at Unzen volcano. In: Yanagi T, Okada H, Ohta K (eds) Unzen volcano, the 1990–1992 eruption. The Nishinippon and Kyushu University Press, Fukuoka, Japan, pp 56–66

Nakada S, Motomura Y (1999) Petrology of the 1991–1995 eruption at Unzen: effusion pulsation and groundmass crystallization. J Volcanol Geotherm Res 89:173–196

Nakada S, Shimizu H, Ohta K (1999) Overview of the 1990–1995 eruption at Unzen volcano. J Volcanol Geotherm Res 89:1–22

Nakada S, Sakuma S, Uto K, Shimizu H, Eichelberger JC (2004) Real images of magmatic conduit: progress of the conduit drilling in Unzen. EOS Trans. AGU 85, Fall Meeting Suppl.: V24B-06

Nonaka M, Nakada S, Goto Y (2004) Emplacement process of the 1991–1995 dome at Unzen volcano, Japan. EOS Trans. AGU 85, Fall Meeting Suppl.:V33D–1486

Papale P (1999) Strain-induced magma fragmentation in explosive eruptions. Nature 397:425–428

Phillips JC, Lane SJ, Lejeune A-M, Hilton M (1995) Gum-rosin-acetone system as an analogue to the degassing behaviour of hydrated magmas. Bull Volcanol 57:263–268

Sato H, Fujii T, Nakada S (1992) Crumbling of dacite dome lava and generation of pyroclastic flows at Unzen volcano. Nature 360:664–666

Smith JV, Miyake Y, Oikawa T (2001) Interpretation of porosity in dacite lava domes as ductile-brittle failure textures. J Volcanol Geotherm Res 112:25–35

Sparks RSJ (1978) The dynamics of bubble formation and growth in Magmas: a review and analysis. J Volcanol Geotherm Res 3:1–37

Sparks RSL (1994) Comment on ”Dynamics of diffusive bubble growth in magmas: isothermal case” by A.A. Proussevitch, D.L Sahagian, and A.T. Anderson. J Geophys Res 99:17827–17828

Sparks RSJ, Barclay J, Calder ES et al (2002) Generation of a debris avalanche and violent pyroclastic density current on 26 December (Boxing Day) at Soufrière Hills Volcano. Montserrat. In: Druitt TH, Kokelaar BP (eds) The eruption of Soufrière Hills Volcano, Montserrat, from 1995 to 1999. Geol Soc Lond Mem 21:409–434

Spieler O, Alidibirov M, Dingwell DB (2003) Grain-size characteristics of experimental pyroclasts of 1980 Mount St. Helens cryptodome dacite: effects of pressure drop and temperature. Bull Volcanol 65:90–104

Spieler O, Dingwell DB, Alidibirov M (2004a) Magma fragmentation speed: an experimental determination. J Volcanol Geotherm Res 129:109–123

Spieler O, Kennedy B, Kueppers U, Dingwell DB, Scheu B, Taddeucci J (2004b) The fragmentation threshold of pyroclastic rocks. Earth Planet Sci Lett 226:139–148

Sugioka I, Bursik M (1995) Explosive fragmentation of erupting magma. Nature 373:689–692

Tuffen H, Dingwell DB, Pinkerton H (2003) Repeated fracture and healing of silicic magma generate flow banding and earthquakes? Geology 31(12):1089–1092

Ui T, Matsuwo N, Suita M, Fujinawa A (1999) Generation of block and ash flows during the 1990–1995 eruption of Unzen Volcano, Japan. J Volcanol Geotherm Res 89:123–137

Umakoshi K, Shimizu H, Matsuwo N, Otha K (1992) Surface temperature measurements of lava domes and pyroclastic flows by infrared thermal video system. In: Yanagi T, Okada H, Ohta K (eds) Unzen Volcano, the 1990–1992 eruption. The Nishinippon and Kyushu University Press, Fukuoka, pp 44–48

Umakoshi K, Shimizu H, Matsuwo N (2001) Volcano-tectonic seismicity at Unzen volcano, Japan 1985–1999. J Volcanol Geotherm Res 112:117–131

Woods AW, Sparks RSJ, Ritchie LJ, Batey J, Gladstone C, Bursik MI (2002) The explosive decompression of a pressurized volcanic dome: the 26 December 1997 collapse and explosion of Soufrière Hills Volcano, Montserrat. In: Druitt TH, Kokelaar BP (eds) The Eruption of Soufrière Hills Volcano, Montserrat, from 1995 to 1999. Geol Soc Lond Mem 21:595–602

Yanagi T, Okada H, Ohta K (1992) Unzen Volcano, the 1990–1992 eruption. The Nishinippon and Kyushu University Press, Fukuoka, 137 pp

Young SR, Sparks RSJ, Aspinall WP, Lynch LL, Miller AD, Robertson REA, Shepherd JB (1998) Overview of the eruption of Soufrière Hills Volcano, Montserrat, 18 July 1995 to December 1997. Geophys Res Lett 25(18):3389–3392

Zhang Y, Sturtevant B, Stolper EM (1997) Dynamics of gas-driven eruptions: experimental simulations using CO2-H2O-polymer system. J Geophys Res 102:3077–3096

Zhang Y (1999) A criterion for the fragmentation of bubbly magma based on brittle failure theory. Nature 402:648–650

Zimanowski B, Büttner R, Lorenz V, Häfele H-G (1997) Fragmentation of basaltic melt in the course of explosive volcanism. J Geophys 102(B1):803–814